

Resonances of a Forced van der Pol Equation with Parametric Damping



Fatemeh Afzali, Ehsan Kharazmi, and Brian F. Feeny

1 Introduction

In this paper, we study the responses of an oscillator with van der Pol terms, parametric damping, and direct excitation. A potential application of this system is a vertical-axis wind-turbine blade, which can endure direct excitation and parametric damping [1, 2], as well as aeroelastic self-excitation, the mechanism of which can be loosely modeled with van der Pol-type nonlinearity [3, 4]. Here, the general behavior of this system is studied, rather than the specific responses of a specific model of an application system. As both parametric excitation and van der Pol nonlinearity can induce instabilities and oscillations, we seek to understand the combined effect of such terms in this system.

Parametric damping has been shown to generate instabilities [2, 5], similar to those of the Mathieu equation [3, 4], with period-1 or period-2 oscillation, and to decay with quasiperiodic dynamics when stable [2]. The study [2] used the Floquet solution combined with harmonic balance [6, 7].

Szabelski and Warminski [8] performed an analytical examinations on the system with three sources of vibration, parametric, self-excited, and inertial. Warminski [9] studied the nonlinear dynamics of a self, parametric, and externally excited oscillator with time delay analytically applying the method of multiple scales. Warminski also discussed the similarities and differences between the van der Pol and Rayleigh for regular, periodic, quasiperiodic, and chaotic oscillations.

F. Afzali (✉) · B. F. Feeny
Michigan State University, East Lansing, MI, USA
e-mail: afzalifa@msu.edu; feeny@egr.msu.edu

E. Kharazmi
Brown University, Providence, RI, USA
e-mail: ehsan_kharazmi@brown.edu

Parametric excitation has also been studied in the context of wind-turbine blades [10–13]. Luongo and Zulli [14] studied a self-excited tower under turbulent wind flow. The tower was assumed to be a nonlinear system where the stationary wind imposed the self-excitation, and the turbulent flow drove both parametric and external excitation. Combining parametric damping with self-excitation of nonlinear damping as in a van der Pol equation, with a particular choice of scaling and excitation frequencies, results in an equation given as

$$\ddot{x} + \epsilon(c_0 + c_1 \cos \omega t + x^2)\dot{x} + \omega_n^2 x = f_0 + f_1 \sin(\omega t), \quad (1)$$

where $\epsilon \ll 1$. The variables c_0 and c_1 are the mean damping and amplitude of the parametric damping, respectively, and f_0 and f_1 are mean and cyclic direct excitation amplitudes. The excitation frequency is ω and the natural frequency is ω_n . We will refer to this as the parametrically damped van der Pol (PDVDP) equation with external excitation.

In this work, we apply the first-order method of multiple scales [3, 15] to study an unforced and externally forced van der Pol equation with parametric damping at frequency ω . We study the sub-harmonic resonance of order $1/2$ as well as the nonresonant dynamics.

2 Perturbation Analysis: Method of Multiple Scales

The core of this study is the approximation of the solution to Eq. (1) based on the method of multiple scale (MMS) [3, 4]. Therefore, we expand the displacement as

$$x(T_0, T_1, \dots) = x_0(T_0, T_1, \dots) + \epsilon x_1(T_0, T_1, \dots) + \epsilon^2 x_2(T_0, T_1, \dots) + \dots, \quad (2)$$

where the time scales are $T_i = \epsilon^i t$, and $\epsilon \ll 1$. By using the chain rule, we obtain the derivatives for $n \in \mathbb{N}$ as $\frac{d^n}{dt^n}(\cdot) = (D_0 + \epsilon D_1 + \epsilon^2 D_2 + \dots)^n(\cdot)$, where $D_i = \frac{\partial}{\partial T_i}$. Here, we carry out the analysis up to the first order by considering the two time scales, $T_0 = t$ and $T_1 = \epsilon t$, and therefore expand the displacement as

$$x(T_0, T_1) \approx x_0(T_0, T_1) + \epsilon x_1(T_0, T_1). \quad (3)$$

By substituting the expansion (3) in Eq. (1) and using the derivatives, coefficients of similar powers of ϵ equate as

$$\epsilon^0 : D_0^2 x_0 + \omega_n^2 x_0 = f_0 + f_1 \sin(\omega t), \quad (4)$$

$$\epsilon^1 : D_0^2 x_1 + \omega_n^2 x_1 = -2D_0 D_1 x_0 - (c_0 + c_1 \cos \omega T_0 + x_0^2)(D_0 x_0). \quad (5)$$

The relationship between the excitation and the natural frequencies specifies different cases of resonance:

1. Nonresonant: no specific relationship between ω and ω_n
2. Primary resonance: $\omega \approx \omega_n$
3. Super-harmonic resonance: $\omega \approx \omega_n/m$ ($m \in \mathbb{N}$)
4. Sub-harmonic resonance: $\omega \approx m\omega_n$ ($m \in \mathbb{N}$)

In the next sections, we elaborate on this perturbation analysis for specific cases with and without external excitation, and apply other tools, to examine the dynamics with emphasis on secondary resonances.

3 Parametric Excitation Without External Excitation

We start with the case where there is no external forcing, i.e. $f_0 = f_1 = 0$. As a survey of the possible dynamics, Fig. 1 shows a frequency sweep from $\omega = 0$ to beyond $\omega = 2\omega_n$, when $\omega_n = 1$, $\epsilon = 0.1$, $c_0 = -1$, and $c_1 = 1$ (these parameters are dimensionless). The sweep, as a bifurcation diagram, is a plot of samples of the x variable of the nonwandering set in a Poincaré section [16] for various values of the frequency parameter. A Runge–Kutta method (Matlab ode45) is used to obtain numerical solutions of several periods to achieve steady-state. As the responses are typically quasiperiodic, the plots are generated by recording at each excitation frequency, 50 values of x at the downward $\dot{x} = 0$ crossing in the phase space.

We appeal to perturbation analysis to explain these responses. The solution to the leading-order Eq. (4) is

$$x_0(T_0, T_1) = A(T_1)e^{i\omega_n T_0} + \text{c.c.}, \tag{6}$$

where c.c. stands for the corresponding complex conjugate terms. We obtain the solvability conditions by substituting Eq. (6) into the right-hand-side of Eq. (5) and eliminating the “secular terms.” In MMS, the secular terms are defined as the terms that make the solution to grow without bound in time, and thus should be eliminated. By plugging Eq. (6) into Eq. (5), we obtain

$$D_0^2 x_1 + \omega_n^2 x_1 = (-2i\omega_n A' - ic_0\omega_n A - i\omega_n A^2 \bar{A})e^{i\omega_n T_0} - \frac{c_1}{2} \left(i\omega_n \bar{A} e^{i(\omega - \omega_n)T_0} \right) + \text{N.S.T.}, \tag{7}$$

where N.S.T stands for non-secular terms and $A' = D_1 A$. The homogeneous solution of Eq. (7) is of the form $e^{i\omega_n T_0}$ and therefore any right-hand-side term that is of the same form will become secular and cause x_1 to grow without bound. We seek the resonance cases that lead to additional secular terms. The right-hand-side of Eq. (7) merely shows the sub-harmonic resonance case. However, as shown in Fig. 1 as well as Eq. (7), the system has significant oscillatory behavior at the nonresonant

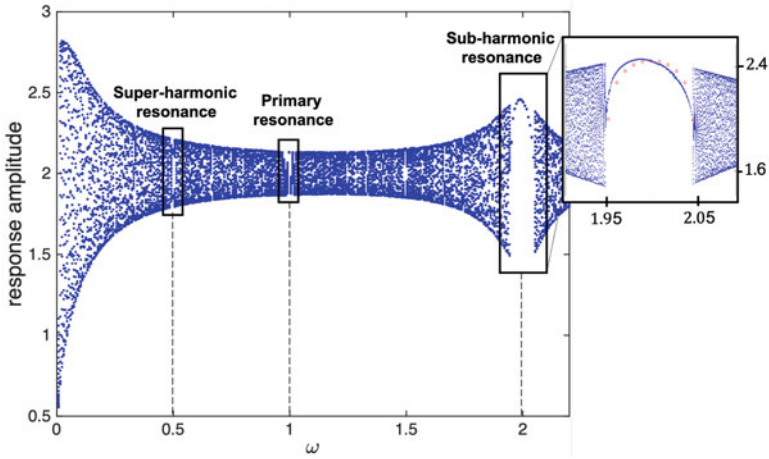


Fig. 1 PDVDP with parametric excitation only. The response amplitude versus the excitation frequency when $f_0 = f_1 = 0$, $\omega_n = 1$, $\epsilon = 0.1$, $c_0 = -1$, and $c_1 = 1$. The embedded sub-plot zooms in on the strong sub-harmonic resonance window. The circles are amplitudes predicted by the perturbation analysis

case, that is when there is no specific relationship between the excitation frequency ω and the natural frequency ω_n .

3.1 Nonresonant Case

We first consider the nonresonant case, where the solvability condition takes the form $2A' + c_0A + A^2\bar{A} = 0$. We recall that A is a complex function of T_1 . Writing it as $A(T_1) = \frac{1}{2}a(T_1)e^{i\beta(T_1)}$, the solvability condition becomes

$$a' + ia\beta' + \frac{1}{2}c_0a + \frac{1}{8}a^3 = 0. \tag{8}$$

By separating the real and imaginary parts, we obtain

$$a' + \frac{1}{2}c_0a + \frac{1}{8}a^3 = 0, \quad a\beta' = 0. \tag{9}$$

The response amplitude has steady-state values that depend on the parameter c_0 and are obtained by setting $a' = 0$. When $c_0 < 0$, there is a stable steady-state amplitude of $a = 2\sqrt{|c_0|}$. This amplitude and the solvability condition that leads to it are the same as in the regular van der Pol equation when $c_0 = -1$.

3.2 Sub-harmonic Resonance of Order 1/2

Here, we focus on the sub-harmonic resonance case, where the excitation frequency is tuned to be close to the double natural frequency, i.e. $\omega = 2\omega_n + \epsilon\sigma$. In this setting, the solvability condition is comprised of more terms and is given as $2A' + c_0A + A^2\bar{A} - \frac{c_1}{2}\bar{A}e^{i\sigma T_1} = 0$. By letting $A(T_1) = \frac{1}{2}a(T_1)e^{i\beta(T_1)}$, we obtain

$$a' + ia\beta' + \frac{1}{2}c_0a + \frac{1}{8}a^3 - \frac{1}{4}c_1ae^{i(\sigma T_1 - 2\beta)} = 0. \tag{10}$$

We separate the real and imaginary parts and then make the system autonomous via the change of variables $\gamma = \sigma T_1 - 2\beta$ to obtain the following governing equations of amplitude a and phase γ as

$$a' + \frac{1}{2}c_0a + \frac{1}{8}a^3 - \frac{1}{4}c_1a \cos(\gamma) = 0, \quad a\gamma' + \frac{1}{2}c_1a \sin(\gamma) - \sigma a = 0. \tag{11}$$

The response amplitude has steady-state values that depend on the parameters c_0 and c_1 and are obtained by setting $a' = \gamma' = 0$. By using the trigonometric identities, we remove γ and finally obtain the response amplitude as

$$a = 0, \quad \text{or} \quad a^2 = -4c_0 \pm 4\sqrt{\frac{c_1^2}{4} - \sigma^2}. \tag{12}$$

If $\frac{c_1^2}{4} - \sigma^2 > 0$, then Eq. (12) indicates that there are both zero and nonzero real-valued response amplitudes. Otherwise, the only steady-state amplitude is zero. Stability of these solutions is determined from the Jacobian of Eqs. (11).

Figure 2 shows the steady-state amplitude versus the excitation frequency $\omega = 2\omega_n + \epsilon\sigma$ for different values of c_0 and c_1 where $\epsilon = 0.1$ and $\omega_n = 1$. By slightly sweeping the detuning parameter σ , we keep the excitation frequency ω close to $2\omega_n$. We observe the emergence of a limit cycle at $\omega \approx 1.95$, whose amplitude grows and then disappears at $\omega \approx 2.05$. When $c_0 = -1$, a larger amplitude of parametric damping c_1 leads to a larger response amplitude; see the left panel in Fig. 2 where the inner and outer ellipses are associated with $c_1 = 0.2$ and $c_1 = 1$, respectively. An increase in the mean value of damping c_0 , however, decreases the response amplitude by moving down the ellipse till the horizontal axis $a = 0$, beyond which the lower branch of ellipse disappears; see the right panel in Fig. 2.

4 Parametric and External Excitation

In this case, the external forcing terms f_0 and f_1 are nonzero. Similar to the previous case, as a survey of the possible dynamics, Fig. 3 shows a frequency sweep from $\omega =$

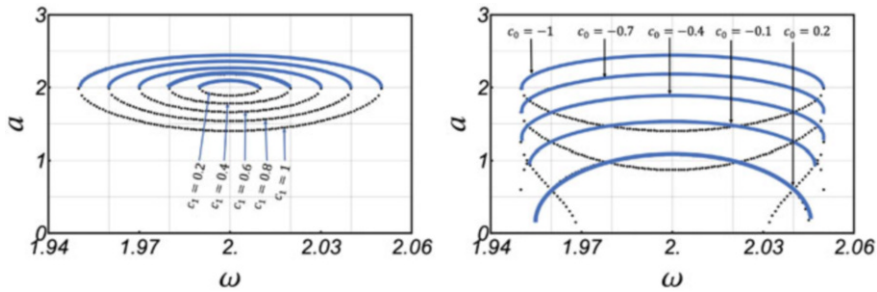


Fig. 2 PDVDP with parametric excitation only: nonzero steady-state response amplitude versus the excitation frequency in the case of sub-harmonic resonance. Left: $c_0 = -1$ and $c_1 = \{0.2, 0.4, 0.6, 0.8, 1\}$. Right: $c_1 = 1$ and $c_0 = \{-1, -0.7, -0.4, -0.1, 0.2\}$. Solid and dotted curves are stable and unstable branches

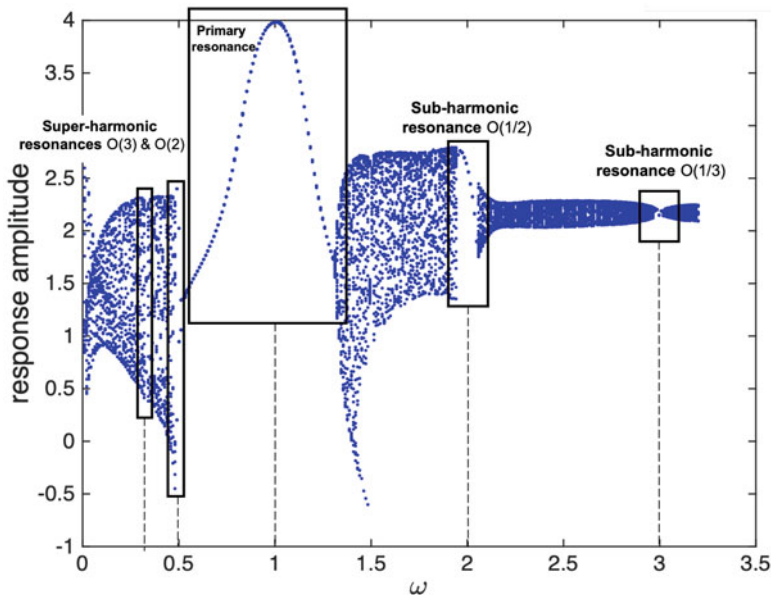


Fig. 3 PDVDP with parametric and external excitation. The response amplitude versus the excitation frequency ω where $f_0 = 0.2$, $f_1 = 1$, $\omega_n = 1$, $\epsilon = 0.1$, $c_0 = -1$, and $c_1 = 1$

0 to beyond $\omega = 3\omega_n$, with parameters $\omega_n = 1$, $c_0 = -1$, $c_1 = 1$, $f_0 = 0.2$, and $f_1 = 1$. The sweep is based on numerical simulations, and the steady-state response amplitudes are plotted. The plot shows that significant quasiperiodic dynamics occur for a large range of excitation frequencies with periodic windows around $\omega \approx \omega_n$, $\omega \approx 2\omega_n$, and $\omega \approx 3\omega_n$. The largest responses occur near the primary resonance range and then for sub-harmonic ones. Super-harmonic resonances are not apparent.

In this case, the particular solution to the leading order Eq. (4) is

$$x_0(T_0, T_1) = \Gamma + i\Lambda e^{i\omega T_0} + A(T_1)e^{i\omega_n T_0} - i\Lambda e^{-i\omega T_0} + \bar{A}(T_1)e^{-i\omega_n T_0}, \quad (13)$$

where $\Gamma = \frac{f_0}{\omega_n^2}$ and $\Lambda = \frac{f_1}{2(\omega^2 - \omega_n^2)}$. By plugging Eq. (13) in Eq. (5), we obtain

$$\begin{aligned} D_0^2 x_1 + \omega_n^2 x_1 = & \left(-2i\omega_n A' - ic_0\omega_n A - i\omega_n \Gamma^2 A - i\omega_n A^2 \bar{A} - 2i\omega_n \Lambda^2 A \right) e^{i\omega_n T_0} \\ & + \left(c_0\omega\Lambda + \omega\Gamma^2\Lambda + \omega\Lambda^3 + 2\omega A\bar{A}\Lambda \right) e^{i\omega T_0} \\ & + \left(\frac{c_1}{2}\omega\Lambda + 2i\omega\Gamma\Lambda^2 \right) e^{2i\omega T_0} \\ & - \omega\Lambda^3 e^{3i\omega T_0} + \left(i\frac{c_1}{2}\omega_n\bar{A} - 2\omega_n\Lambda\Gamma\bar{A} + 2\omega\Lambda\Gamma\bar{A} \right) e^{i(\omega - \omega_n)T_0} \\ & + i(2\omega - \omega_n)\Lambda^2\bar{A}e^{i(2\omega - \omega_n)T_0} + (\omega - 2\omega_n)\Lambda\bar{A}^2e^{i(\omega - 2\omega_n)T_0} \\ & + \text{c.c.} + \text{N.S.T.} \end{aligned} \quad (14)$$

The right-hand-side of Eq. (14) shows different cases of resonance; each can produce different secular terms. The cases are nonresonant, sub-harmonic resonance of orders 1/2 and 1/3, and super-harmonic resonance of order 2. Here we study the first two cases. The third case (super-harmonic of order 1/3) does not involve the parametric term, and others turn out to be of minimal significance. For the first two cases, we obtain the following solvability conditions:

- Nonresonant:

$$2A' + c_0A + \Gamma^2A + A^2\bar{A} + 2\Lambda^2A = 0 \quad (15)$$

- Sub-harmonic Resonance of Order 1/2 ($\omega \approx 2\omega_n$):

$$2A' + c_0A + \Gamma^2A + A^2\bar{A} + 2\Lambda^2A - \left(\frac{c_1}{2} - 2i\Lambda\Gamma \left(\frac{\omega}{\omega_n} - 1 \right) \right) \bar{A}e^{i\sigma T_1} = 0. \quad (16)$$

Although Fig. 3 indicates the primary resonance as a prominent case when $\omega \approx \omega_n$, the coefficient Λ becomes singular and would contradict the multiple-scales bookkeeping strategy. The analysis of primary resonance case requires weak excitation, as well as a second-order perturbation analysis to capture the parametric term, as in [17]. This will be analyzed in a separate study.

4.1 Nonresonant Case

The solvability condition in Eq. (15) is not affected by the parametric damping term, and hence the behavior is similar to the forced van der Pol equation [3, 4]. In this case, the phase equation becomes $\beta' = 0$, and hence the phase β is constant and does not influence the oscillation frequency. The amplitude equation yields the following steady-state solutions:

$$a = 0, \quad a = 2\sqrt{-c_0 - \Gamma^2 - 2\Lambda^2}, \tag{17}$$

where the zero solution is unstable and the nonzero solution exists and is stable when $\Gamma^2 + 2\Lambda^2 < -c_0$. Since $\Gamma^2 + 2\Lambda^2 > 0$, a negative value of c_0 is necessary (but not sufficient) for nonzero a . If the above condition is not satisfied, then the trivial solution $a = 0$ is stable.

Since the leading-order solution has the form

$$x_0 = \Gamma - 2\Lambda \sin \omega T_0 + a \cos(\omega_n T_0 + \beta) \tag{18}$$

when the condition $\Gamma^2 + 2\Lambda^2 < -c_0$ is satisfied, $a \neq 0$ and the response becomes quasiperiodic. Otherwise, with sufficient increase in the excitation (Λ and Γ), a is suppressed and the response becomes periodic; known as quenching [3, 4].

The parametric terms affect the first-order correction, x_1 , in the approximate solution $x(t) = x_0(t_0, T_1) + \epsilon x_1(T_0, T_1)$. In eliminating the secular terms, there are several contributions of different frequency components, including $2\omega, \omega - \omega_n, \omega + \omega_n$, from parametric excitation and van der Pol terms, and $2\omega_n, 3\omega_n, 3\omega, 2\omega - \omega_n, 2\omega + \omega_n, \omega - 2\omega_n$, and $\omega + 2\omega_n$, from the van der Pol terms. Thus the first-order solution can contribute two-frequency quasiperiodic effects, as the content of the total response has a linear combination of two frequencies.

4.2 Sub-harmonic Resonance of Order 1/2

In this case, the excitation and natural frequency form the relation $\omega = 2\omega_n + \epsilon\sigma$. We see from the solvability condition in Eq. (16) that in addition to the nonresonant secular terms in Eq. (15), the parametric damping and forcing appear. We substitute $A(T_1) = \frac{1}{2}a(T_1)e^{i\beta(T_1)}$ into the equation and let $\gamma = \sigma T_1 - 2\beta$. Then, the autonomous coupled system of governing equations of the amplitude a and phase γ becomes

$$\begin{aligned} a' + \frac{1}{8}a^3 + \left(\frac{c_0}{2} + \frac{\omega_n \Gamma^2}{2} + \Lambda^2 - \frac{c_1}{4} \cos \gamma + \Gamma \Lambda \left(1 - \frac{\omega}{\omega_n} \right) \sin \gamma \right) a &= 0, \\ a\gamma' - a\sigma + \frac{c_1}{2}a \sin \gamma + 2a\Gamma \Lambda \left(1 - \frac{\omega}{\omega_n} \right) \cos \gamma &= 0. \end{aligned} \tag{19}$$

The fixed points of Eq. (19) are obtained in the steady-state case when $a' = \gamma' = 0$, which admits $a = 0$ and a nontrivial solution. The equations for the nontrivial solution take the form $A_1 \sin \gamma + B_1 \cos \gamma = C_1$ and $A_2 \sin \gamma + B_2 \cos \gamma = C_2$ where the coefficients A_1, A_2, B_1, B_2, C_1 , and C_2 are functions of the parameters and the amplitude a . By solving for $\sin \gamma$ and $\cos \gamma$, and using the trigonometric identities, we remove the variable γ and form a parametric algebraic equation to

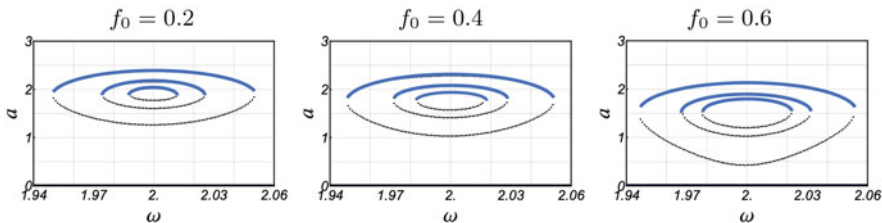


Fig. 4 PDVDP with parametric and external excitation in the case of sub-harmonic resonance where $c_0 = -1$ and $f_1 = 1$. The three plotted curves correspond to $c_1 = \{0.2, 0.5, 1\}$, and the panels are for $f_0 = \{0.2, 0.4, 0.6\}$. Solid and dotted curves are stable and unstable branches

obtain the steady-state amplitude a as,

$$a^4 + 8a^2(c_0 + 2\Lambda^2 + \Gamma^2) + 4(4c_0^2 + 16c_0\Lambda^2 - c_1^2 + 16\Lambda^4 + 4\sigma^2) + 16\Gamma^2 \left(2c_0 - 4\Lambda^2 \frac{\omega}{\omega_n} \left(\frac{\omega}{\omega_n} - 2 \right) + \Gamma^2 \right) = 0. \tag{20}$$

Solving for a^2 yields the steady-state response amplitude, which is valid if the square root in the quadratic-equation solution is real, and if $a^2 \geq 0$. The first criterion reduces to $4\sigma^2 < c_1^2 + 16\Gamma^2\Lambda^2$, when using $\omega - \omega_n \approx \omega_n$. Thus the frequency range of fixed amplitude solutions increases with c_1 , f_0 , and f_1 . For the case in which a and γ are fixed and stable, based on Eq. (13) and the definition of γ , the leading order solution takes the form

$$x_0 = \Gamma - 2\Lambda \sin(\omega T_0) + a \cos\left(\frac{\omega}{2}T_0 - \frac{\gamma}{2}\right), \tag{21}$$

which is a periodic (phase locked) response of fundamental frequency $\omega/2$. When a steady-state solution a does not exist, the response is in phase drift, and is quasiperiodic.

Figure 4 shows the steady-state response amplitude versus the excitation frequency for small value of detuning parameter, when $\epsilon = 0.1$ and $-0.5 < \sigma < 0.5$. Note that these figures show the amplitude a of one term in Eq. (21). The phase γ would affect peak-to-peak amplitudes. The mean damping and periodic forcing are set to be constant, $c_0 = -1$ and $f_1 = 1$, while different values of $c_1 = \{0.2, 0.5, 1\}$ are showing the ellipses. The larger values of c_1 are associated with the larger ellipses. We see that as the constant forcing term f_0 is varying between $\{0.2, 0.4, 0.6\}$, the ellipses are distorted and the limit cycle amplitude is increased. The sub-harmonic behavior of the parametric plus direct excitation is thus similar to that of the parametric excitation only, except that the solutions for the steady amplitudes are complicated and distorted by the direct excitation terms f_0 and f_1 .

5 Summary and Conclusions

In this paper, we studied the resonance of a forced and unforced van der Pol equation with parametric damping. Applications can include vertical-axis wind-turbine blade vibration, which can have parametric damping and van-der-Pol type terms in simplified models. The first-order method of multiple scales and numerical solutions were used.

The parametric damping with no external excitation demonstrated nonresonant and sub-harmonic resonance cases, where the system shows an oscillatory quasiperiodic behavior in the former case. In the latter resonance case, we found the steady-state amplitude versus the excitation frequency for different damping parameters. When $c_0 = -1$ (negative linear damping as with the van der Pol oscillator), the resonant response amplitude increases with the parametric damping c_1 . An increase in the mean value of damping c_0 , however, decreases the response amplitude.

We then studied van der Pol with parametric and direct excitation. In the nonresonant case the parametric damping term does not contribute in the solvability condition and therefore it showed the same behavior as the forced van der Pol. The nonresonant system can exhibit the quenching phenomenon when the excitation through the direct forcing is sufficiently large.

Our numerical studies showed the primary resonance as a dominant forced response case. The analysis of this case requires further investigation that will be done as a subsequent study with weak excitation. Based on previous studies on the cases with forcing and cyclic stiffness [17], we expect that a second-order multiple-scales analysis should be considered to correctly pull out the contribution of the parametric damping to the different resonance cases.

References

1. F. Afzali, O. Kapucu, B.F. Feeny, Vibrational analysis of vertical-axis wind-turbine blades, in *Proceedings of the ASME 2016 International Design Engineering Technical Conferences*. Paper number IDETC2016-60374, Charlotte, North Carolina, August 21–24 (2016)
2. F. Afzali, G.D. Acar, B.F. Feeny, A Floquet-based analysis of parametric excitation through the damping coefficient. *J. Vib. Acoust.* **143**(4), 041003 (2021)
3. A.H. Nayfeh, D.T. Mook, *Nonlinear Oscillations* (Wiley, New York, 2008)
4. R.H. Rand, *Lecture Notes on Nonlinear Vibrations* (2012). <https://ecommons.cornell.edu/handle/1813/28989>
5. Hartono, and A.H.P. Burgh, *An Equation Time-periodic Damping Coefficient: Stability Diagram and an Application* (Delft University of Technology, Delft, 2002)
6. G. Acar, B.F. Feeny, Floquet-based analysis of general responses of the Mathieu equation. *J. Vib. Acoust.* **138**(4), 041017(9 pages) (2016)
7. F. Afzali, B.F. Feeny, Response characteristics of systems with parametric excitation through damping and stiffness, in *In ASME International Design Engineering Technical Conferences and Computers and Information in Engineering Conference, American Society of Mechanical Engineers* (2020). paper number DETC2020-22457

8. K. Szabelski, J. Warmiński, Parametric self-excited non-linear system vibrations analysis with inertial excitation. *Int. J. Non Linear Mech.* **30**(2), 179–189 (1995)
9. J. Warminski, Nonlinear dynamics of self-, parametric, and externally excited oscillator with time delay: van der pol versus Rayleigh models. *Nonlinear Dyn.* **99**(1), 35–56 (2020)
10. V. Ramakrishnan, B.F. Feeny, Resonances of a forced Mathieu equation with reference to wind turbine blades. *J. Vib. Acoust.* **134**(6), 064501 (2012)
11. M.S. Allen, M.W. Sracic, S. Chauhan, M.H. Hansen, Output-only modal analysis of linear time-periodic systems with application to wind turbine simulation data. *Mech. Syst. Sig. Process.* **25**(4), 1174–1191 (2011)
12. T. Inoue, Y. Ishida, T. Kiyohara, Nonlinear vibration analysis of the wind turbine blade (occurrence of the superharmonic resonance in the out of plane vibration of the elastic blade). *J. Vib. Acoust.* **134**(3), 031009 (2012)
13. G.D. Acar, M.A. Acar, B.F. Feeny, Parametric resonances of a three-blade-rotor system with reference to wind turbines. *J. Vib. Acoust.* **142**(2), 021013(9 pages) (2020)
14. A. Luongo, D. Zulli, Parametric, external and self-excitation of a tower under turbulent wind flow. *J. Sound Vib.* **330**(13), 3057–3069 (2011)
15. A.H. Nayfeh, *Perturbation Methods* (Wiley, New York, 2008)
16. J. Guckenheimer, P. Holmes, *Nonlinear Oscillations, Dynamical Systems, and Bifurcations of Vector Fields* (Springer, New York, 1983)
17. V. Ramakrishnan, Analysis of wind turbine blade vibration and drivetrain loads. PhD thesis (Michigan State University, East Lansing, 2017)